

Novel Near-Field Microwave Bone Healing Monitoring Using Open-Ended Rectangular Waveguides

Akram S. Bin Sediq, Nasser Qaddoumi and Hasan Al-Nashash

American University of Sharjah, School of Engineering, Electrical Engineering Department,
Sharjah, P. O. Box: 26666, UAE.

Abstract — In this paper, results of the simulated interaction of microwaves in the near-field region of a waveguide with a fractured Tibia are presented. The Tibia bone fracture is one of the most difficult fractures to treat because of the slow healing process which may take up to 5 months. The human body is modeled as a three layer medium: skin, fasciae with fat, muscle and bone. Each of these layers is characterized by its dielectric properties. These properties influence the incident, transmitted and reflected waves. In this paper, simulation results of Tibia bone healing monitoring using an X-band open ended rectangular waveguide operating in the near-field region at microwave frequencies are presented. An extensive optimization process was performed to arrive at optimal measurement parameters. Frequency of operation and the material that fills the waveguide were investigated to improve the sensitivity of detection and to monitor five different stages of the healing process. Both phase images and radiation patterns show that using rectangular waveguides has great potential in monitoring the healing process of the Tibia bone.

Index Terms — Bone Healing monitoring, Microwave NDT, Waveguide, Microwave Imaging.

I. INTRODUCTION

When a bone is fractured, partial or complete break in the continuity of the bone occurs. This happens under mechanical stress that exceeds the limits of the bone's strength and stiffness [1]. A Bone fracture causes a sudden loss of bone continuity, stability and integrity. A fracture usually interrupts or cuts the blood vessels which causes a reduction of blood supply. One to two mm of bone dies on either side of the fracture due to the lack of blood supply. Treatment usually involves reduction or realignment of the bone, immobilization and restoring function through rehabilitation. The healing process starts when new bone (callus layer) forms and fills in the fractured area to restore the original continuity and solidity. It generally goes through the same series of stages for all fractures: inflammation, soft tissue formation, hard tissue formation, new bone and remodeling [2]. As healing progresses, the callus layer begins to disappear. Consequently, by monitoring the decay of the callus layer thickness, bone healing stage may be quantitatively estimated. Healing is considered to be complete when the bone is almost identical to its original shape before injury and has regained its normal stiffness and strength.

A bone fracture may be diagnosed by many diagnostic imaging tests such as X – Rays, Computed Tomography (CT), Magnetic Resonance Imaging (MRI) or Vibratory devices [3-5]. Since the bone healing process may take several months in certain pathological cases, repetitive tests are required. X – Ray radiation is hazardous and is unsafe for such repetitive tests. Moreover, fractures are typically visible on primary radiographs. However, the healing process' Soft Tissue stage is difficult to visualize on radiographs. In other words, the fracture site is seen on an X-ray like a cloudy area. It becomes visible after three to six weeks after injury. Furthermore, X-rays can not be used for pregnant women or patients who had a barium contrast media or any medication containing bismuth.

MRI tests are long and of high cost and can not be repetitive. The MRI machine itself is prohibitively expensive for small hospitals and therefore, it is not available everywhere. Additionally, people who are claustrophobic, nervous, or disturbed by the loud noise caused by MRI machines must be given some anti-anxiety medication before the examination.

Vibratory devices are mechanical sine wave vibrators that are applied to the fracture site [5]. An electromagnetic shaker is pushed against the skin near the distal end of the bone. A miniature accelerometer captures the response of the bone-prosthesis system to the applied vibrations. If there is no fracture, the bone system behaves linearly and only the excitation frequency will be detected. However, if there is fracture, the system will behave in a non-linear mode and harmonics will be detected by the accelerometer. Experiments have shown that an excitation frequency between 100 Hz to 200 Hz is well suited to detect fractures. Unfortunately however, vibratory devices suffer from the increased signal damping and locating the resonance frequency especially with obese subjects. Recently, the potential of utilizing Ultrasound was demonstrated as a tool to monitor the healing process of the Tibia [6].

Microwave near field non-destructive testing utilizing open ended rectangular waveguide has not been used, thus far, in detecting bone fracture rather than monitoring of the bone healing process.

In microwave NDT systems, the testing is accomplished by illuminating the inspected material with electromagnetic waves. Both magnitude and phase of

the reflected/transmitted waves carry information about the properties of the defect. By monitoring these waves information about the integrity of the specimen under inspection may be obtained. This work is devoted to study the feasibility of using this technique in monitoring the bone healing process through theoretical simulations and then the results will be compared with those obtained using ultrasound.

II. THEORETICAL BACKGROUND

In this paper, two mathematical models are proposed to model and simulate the interaction between an open-ended rectangular waveguide operating in the near-field at microwave frequencies with biological tissue during the bone healing process. The first model calculates the reflection coefficient at the aperture of a waveguide operating at any frequency and illuminates an N-layer structure. Consider the dominant TE₁₀ mode incident on the waveguide aperture, the terminating admittance of the waveguide can be written as [7]:

$$Y = G + jB$$

$$= \frac{\iint_{\text{aperture}} [\vec{E}(x, y, 0) \times \vec{W}(x, y, 0)] \hat{a}_z dx dy}{\left[\iint_{\text{aperture}} \vec{E}(x, y, 0) \cdot \vec{e}_o(x, y) dx dy \right]^2} \quad (1)$$

Where

$$\vec{W}(x, y) = \vec{H}(x, y, 0) + \sum_{n=0}^{\infty} Y_n \vec{h}_n(x, y) \iint_{\text{aperture}} \vec{E}(\eta, \xi, 0) \cdot \vec{e}_n(\eta, \xi) d\eta d\xi \quad (2)$$

Where $E(x, y, 0)$ and $H(x, y, 0)$ are the electric and magnetic field distributions, respectively. The admittance expression is constructed using transverse vector mode functions and their orthogonal properties. The n^{th} vector mode functions are e_n , and h_n , and Y_n is the characteristic admittance of the waveguide for the n^{th} mode. The broad and narrow dimensions of the waveguide are a and b , respectively. Hence, the TE₁₀ mode aperture field distribution is given by

$$E_y(x, y, 0) = \vec{e}_o(x, y) = \begin{cases} \sqrt{\frac{2}{ab}} \cos\left(\frac{\pi x}{a}\right) & (x, y) \in \text{aperture} \\ 0 & (x, y) \notin \text{aperture} \end{cases} \quad (3)$$

The complex reflection coefficient at the aperture of the waveguide is related to the terminating admittance of the waveguide, Y , by

$$\Gamma = |\Gamma| e^{j\phi} = \frac{I - Y}{I + Y} \quad (4)$$

Which is a complex quantity whose phase and magnitude variations can be calculated and measured for testing and assessment.

The second model calculates the radiation pattern inside N-layered structure. To find the power at every point inside the N-layered structure, both the electric field and magnetic field must be calculated first. The electric and magnetic fields are calculated using:

$$\vec{E}(x, y, z) = \int_{-\infty}^{\infty} \int_{-\infty}^{\infty} \vec{F}(k_x, k_y, z) e^{j(k_x x + k_y y)} dk_x dk_y \quad (5)$$

$$\vec{H}(x, y, z) = \int_{-\infty}^{\infty} \int_{-\infty}^{\infty} \vec{L}(k_x, k_y, z) e^{j(k_x x + k_y y)} dk_x dk_y \quad (6)$$

Where

$$\vec{F} = (A_x \hat{x} + A_y \hat{y} + \frac{jk_x A_x + jk_y A_y}{\gamma} \hat{z}) e^{-\gamma z} + (B_x \hat{x} + B_y \hat{y} + \frac{-jk_x B_x - jk_y B_y}{\gamma} \hat{z}) e^{\gamma z}$$

$$\vec{L}(k_x, k_y, z) = \frac{j}{\omega \mu_n} \{ [\hat{x}(-C_z A_x - C_x A_y) + \hat{y}(C_y A_x + C_z A_y) + \hat{z}(-jk_y A_x + jk_x A_y)] e^{-\gamma z} + [\hat{x}(C_z B_x + C_x B_y) + \hat{y}(-C_y B_x - C_z B_y) + \hat{z}(-jk_y B_x + jk_x B_y)] e^{\gamma z} \}$$

$$\gamma = \sqrt{k_x^2 + k_y^2 - K^2}$$

$$C_x = \frac{K^2 - k_x^2}{\gamma}, \quad C_y = \frac{K^2 - k_y^2}{\gamma}, \quad C_z = \frac{k_x k_y}{\gamma}$$

The details of this model can be found in [8].

Both models were used to find the optimum operating frequency and optimum dielectric constant of the waveguide filling material. This is in addition to obtaining the radiation pattern with and without the callus layer and to generate theoretical images for different stages in the healing process.

III. SIMULATIONS AND RESULTS

In this section, we present the results of the two models described earlier. the optimization procedure. Figure 1 shows an X-band rectangular waveguide radiating into a 4-layered stratified structure. The

dielectric properties of each layer depend non-linearly on the frequency of operation. A curve fitting formula was used to calculate the complex dielectric constant of each layer (ϵ_r) at different frequencies [9]. To find the optimum frequency of operation and the optimum material to fill the waveguide, an extensive investigation was conducted using an X-band rectangular waveguide with dimensions of $a = 2.286$ cm and $b = 1.016$ cm operating in the dominant mode TE_{10} . The target was to find the maximum difference in either magnitude or phase of the reflection coefficient between the case of no callus (bone is healed) and the case of maximum callus (0.2 mm at the beginning of healing). As shown in figure 2, the difference in the calculated magnitude of the reflection coefficient improves with loading the waveguide and has a maximum value of 0.0098 when ϵ_r of the filling material is $32-j0$ at a frequency of 1.28 GHz. However, practically, the minimum difference in the magnitude of the reflection coefficient that can be measured is 0.01. Consequently, measurements of the magnitude are not adequate for this application. Figure 3 shows the difference in the phase of the reflection coefficient as it improves with loading the waveguide. The figure shows that 4.5 degrees of phase difference may be measured when ϵ_r of the filling material is $20-j0$ at a frequency of 1.6 GHz. The minimum phase difference that can be measured practically is 0.5 degrees, which implies that measuring the phase at this frequency will lead to a reliable detection of the healing stage. We remark that changing the material that fills the waveguide will lead to a change in the frequency range of the dominant mode. This allowed us to operate at lower frequency and hence minimum attenuation in such a lossy structure. Moreover, loading the waveguide improved the coupling of the microwave signal to the body.

The inspected structure was modeled as described below:

Layer 1: Skin, $\epsilon_r = 41.7 - 12.6j$, thickness: 1.2 mm.

Layer 2: Fasciae & Fat, $\epsilon_r = 5.4 - 0.8j$, thickness: 1.0 mm.

Layer 3: this layer is a fat layer with a thickness of 0.2 mm except for a small circular area (1 cm²) where the fat is replaced by callus (with properties like bone). The callus thickness is estimated to be 0.2 mm at the beginning and decays to 0.0 mm when the healing is

complete. The thickness of the callus depends on the healing stage. Consequently, monitoring this callus layer reveals information about the healing stage.

Layer 4: bone, $\epsilon_r = 11.9 - 2.7j$, thickness: infinite half-space (usually 3 mm thick).

Figure 4 shows the real power radiation pattern for the case when the bone is totally healed (No callus layer) and for the case of beginning of healing (thickness of callus layer is 0.2 mm). It is clear that the presence of the callus layer altered the power distribution. This shows that the reflected signals obtained from the two cases are different. This suggests that measuring the reflection coefficient, or a signal proportional to it, will lead to the detection of the bone healing stage.

As mentioned before, our objective is to monitor the bone healing process through measurement of the thickness of the callus layer. Figure 5 shows the phase as a function of the callus layer thickness. The phase changes linearly with the thickness of the callus layer, this is extremely important from the practical point of view. It means that quantifying the healing stage is possible due to the linear behavior. Since the minimum change in phase that can be detected practically is 0.5 degrees, and we have a total dynamic range of 4.5 degrees, we can relatively easily distinguish among five different healing stages. Figures 6.a to 6.e show the theoretical phase images for different thicknesses of the callus layer and hence different stages of the healing process. All images have the same color scale. It is apparent from the theoretical images that we can, with the proposed system, distinguish clearly five different stages.

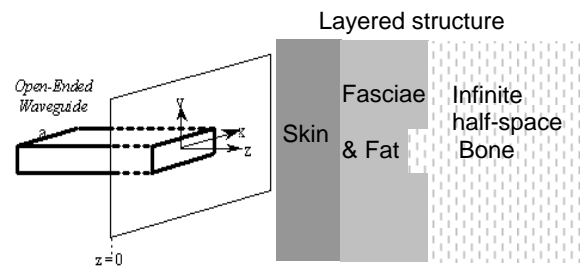


Figure 1: The cross-section of an open-ended rectangular waveguide radiating into a 4-layer structure.

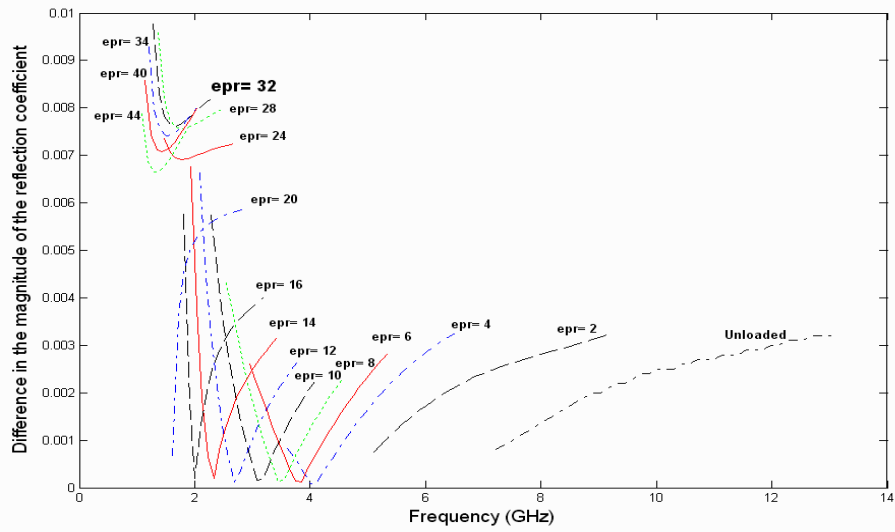


Figure 2: The difference of the magnitude of the reflection coefficient between the two cases of fracture and no fracture as a function of the operating frequency for different ϵ_r of the material that fills an X-band rectangular waveguide.

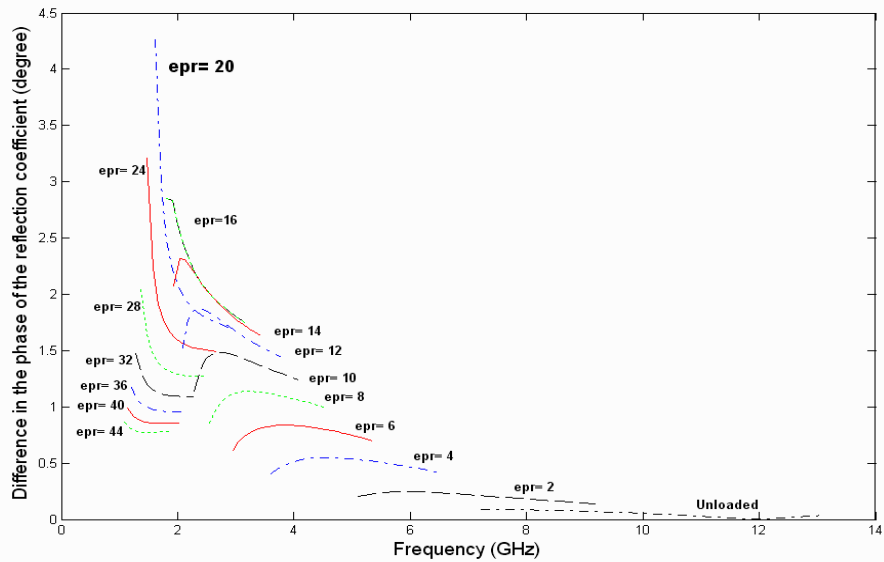


Figure 3: The difference of the phase of the reflection coefficient between the two cases of fracture and no fracture as a function of the operating frequency for different ϵ_r of the material that fills an X-band rectangular waveguide.

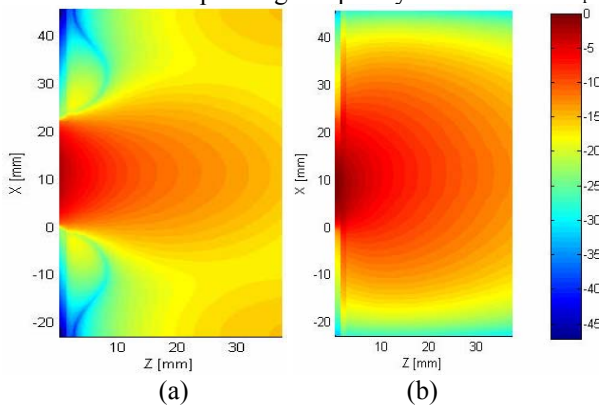


Figure 4: Real power pattern (dB) in the xz plane at $y=b/2$ a) No callus and b) Maximum callus.

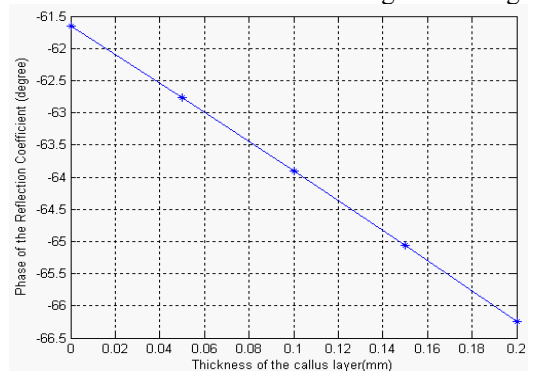


Figure 5: The phase of the reflection coefficient for different thicknesses of the callus layer.

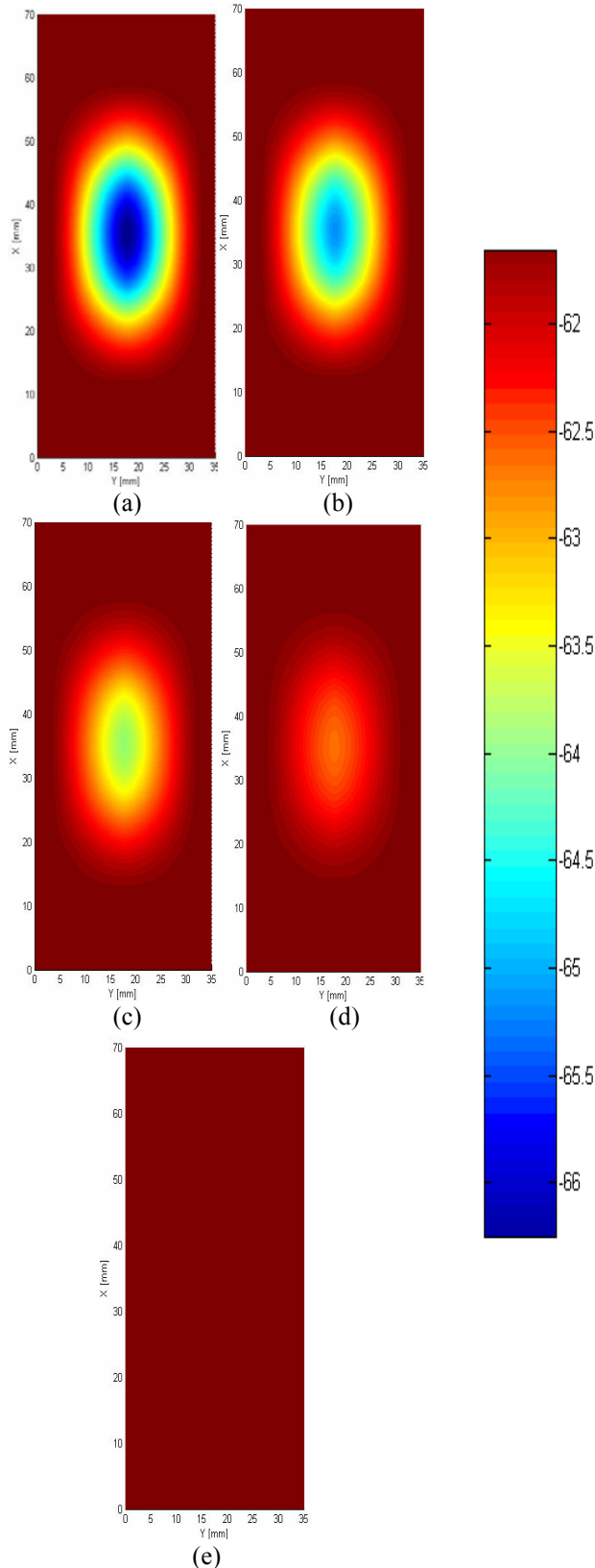


Figure 6: Theoretical phase images when the thickness of the callus layer is a) 0.2 mm (0% healing), b) 0.15 mm (25% healing), c) 0.10 mm (50% healing), d) 0.05 mm (75% healing), e) 0.00 mm (100% healing).

IV. CONCLUSIONS

The simulation results of the power patterns accompanied with the theoretical images, demonstrated the potential of near field microwave non destructive testing utilizing open ended loaded rectangular waveguide in monitoring the bone healing process of the Tibia. Through optimization, an X-band rectangular waveguide loaded with a mixture that has ϵ_r of 20-0j operating at a frequency of 1.6 GHz, can distinguish five different stages of the healing process. Future work will include using standoff distance as well as the dielectric material to be inserted between the waveguide and the inspected structure as other optimization parameters to improve the dynamic range and to be able to distinguish more than five different stages.

REFERENCES

- [1] G. Thibodeau and K. Patton, "Anatomy and Physiology," Mosby, 4th edition, 1999.
- [2] R. Johnston, "Problems That Can Occur During Fracture Healing", <http://www.hughston.com/hha/a.fracture.htm>
- [3] A. Webb, "Introduction to Biomedical Imaging", IEEE Press Series and John Wiley and Sons, 2003.
- [4] R. Colier and R. Donarski, "on-invasive method of measuring the resonant frequency of a human tibia in vivo", Part 1 & 2, J Biomed Eng, pp. 9:321-331, 1987.
- [5] R. Collier, R. Donarski, A. Worley and A. Lay. "The use of externally applied mechanical vibrations to assess both fractures and hip prosthesis" Chapter 18, pp. 151-163 in Turner Smith, A.R. (ed.), Micromovement in Orthopaedics. Oxford University Press., 1993.
- [6] A. Hijazy, H. Al – Smoudi, M. Swedan, H. Al – Nashash, N. Qaddoumi, and K.G. Ramesh "Quantitative Monitoring of Bone Healing Process Using Ultrasound," Proceedings of the First International Conference on Modeling, Simulation and Applied Optimization, Sharjah, U.A.E. February 1-3, 2005.
- [7] N. Qaddoumi, "Microwave Detection and Characterization of Subsurface Defect Properties in Composites Using Open Ended Rectangular Waveguide," Ph.D. Dissertation, Colorado State University, 1998.
- [8] A. Bin Sediq, W. Saleh, M. Abou-Khousa and N. Qaddoumi, "Near-Field Radiation Pattern Characteristics of Open-Ended Waveguide Probes," the 2nd IEEE-GCC 2004 Conference, 23-25 November 2004, Gulf International Convention and Exhibition Center, Manama, Bahrain.
- [9] C. Gabriel, "A compilation of the dielectric properties of body tissues at RF and microwave frequencies," Radiofrequency Radiation Division, Brooks AFB, San Antonio, TX, Contract AL/OE-TR-1996-0037, 1996.